CONF-9511184--1

LA-UR- 95-4299

Title: THE INFLUENCE OF MELTING PROCESS AND PARAMETERS ON THE STRUCTURE AND HOMOGENEITY OF TITANIUM-TANTALUM ALLOYS

Author(s): P. S. Dunn, D. Korzewka, F. Garcia

Submitted to: Int'l Conf. on Tungsten and Refractory Metals, Washington, DC
November 15-17, 1995

Los Alamos
NATIONAL LABORATORY

Form No. 836 R5
ST 2629 10/91

THE INFLUENCE OF MELTING PROCESSES AND PARAMETERS ON THE STRUCTURE AND HOMOGENEITY OF TITANIUM-TANTALUM ALLOYS

Paul S. Dunn, Deniece Korzekwa, and Fermin Garcia

Materials Science and Technology Division
Los Alamos National Laboratories*
Los Alamos, New Mexico 87545

Brian K. Damkroger, Jim A. Van Den Avyle, and Ralph G. Tissot

Materials and Processes Science Center
Sandia National Laboratories*
Albuquerque, New Mexico 87185

ABSTRACT

Alloys of titanium with refractory metals are attractive materials for applications requiring high temperature strength and corrosion resistance. However, the widely different characteristics of the component elements have made it difficult to produce sound, compositionally homogeneous ingots using traditional melting techniques. This is particularly critical because the compositional ranges spanned by the micro- and macrosegregation in theses systems can easily encompass a number of microconstituents which are detrimental to mechanical properties. This paper presents the results of a study of plasma (PAM) and vacuum-arc (VAR) melting of a 60 wt% tantalum, 40 wt% titanium binary alloy. The structural and compositional homogeneity of both PAM consolidated + PAM remelted, and PAM consolidated + VAR remelted ingots were characterized and compared using optical and electron microscopy and x-ray fluorescence microanalysis. Additionally, the effect of melting parameter, including melt rate and magnetic stirring, was studied. The results indicate that PAM remelting achieves more complete dissolution of the starting electrode, due to greater local superheat, than does VAR remelting. PAM remelting also produces a finer as-solidified grain structure, due to the smaller molten pool and lower local solidification times. Conversely, VAR remelting produces an ingot with a more uniform macrostructure, due to the more stable movement of the solidification interface and more uniform material feed rate. Based on these results, a three-step process of PAM consolidation, followed by a PAM intermediate melt and a VAR final melt, has been selected for further development of the alloy and processing sequence.

INTRODUCTION AND BACKGROUND

An alloy development program was initiated at Los Alamos to produce an alloy resistant to attack by molten plutonium and having good oxidation resistance, both over a range of temperatures from 800 to 1200°C, in air, and for times of up to several hours. In addition, the material required good room-temperature ductility and high-temperature strength, and was further constrained by the requirement that its density be between 6 and 8 g/cc. The work has centered on tantalum-base because tantalum is known to resist liquid plutonium attack. However, although tantalum works well in the vacuum induction melting of plutonium, its oxidation resistance at 1000°C in air is very poor. The oxidation resistance of tantalum is greatly improved with the addition of titanium as seen

* This work was funded by the Department of Energy under contracts W-7405-ENG-36 and DE-AC04-94AL-85000.
* This work was funded by the Department of Energy under contracts W-7405-ENG-36 and DE-AC04-94AL-85000.

in Figure 1, leading the study to focus on the Ta-Ti binary system (1). Additionally, metallographic characterization of the liquid plutonium attack on electron beam welded titanium-tantalum couples suggested that the alloy system was resistant to plutonium attack.

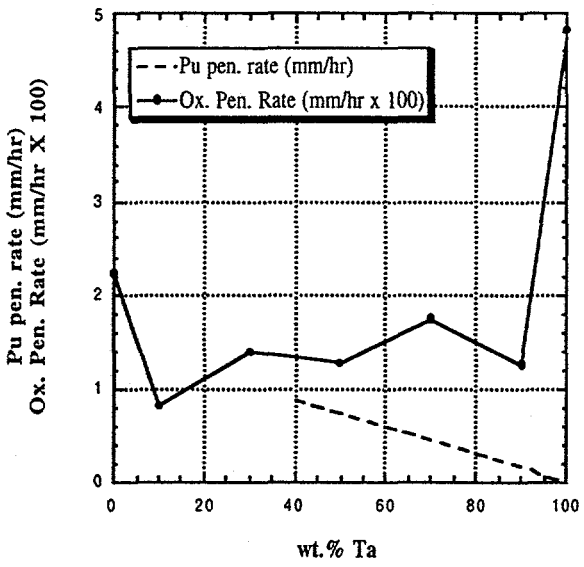

Figure 1. Penetration rates, Pu and O in Ti-Ta binary alloys (1, 2).

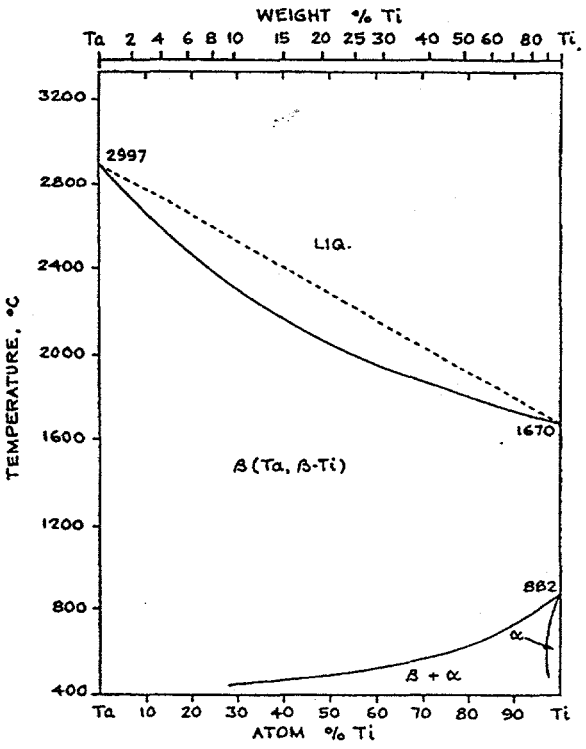

Figure 2. Tantalum-titanium binary phase diagram (1).

Initial studies concentrated on alloys ranging from 10 to 60 wt% tantalum, with 60% being the upper limit due to the density requirements. Small quantities (100g) of test alloys were produced in a nonconsumable arc furnace and screened for depth of molten plutonium attack. The plutonium attack data, which confirms that this is an acceptable alloy system for the desired application, is shown in Figure 1 as well (2). As shown in Figure 1, oxidation resistance is relatively constant from 10 to 90% Ta, but attack by molten Pu decreases with increasing Ta content. These data led to the selection of an alloy having 60 wt% Ta for further studies.

Although the fabrication of small quantities of material was relatively simple, production of full-scale alloy ingots posed major obstacles. The Ti-Ta binary phase diagram, Figure 2, shows that the liquidus and solidus of the alloy are approximately 1950°C and 2100°C, respectively, and that the melting temperatures of the Ti and Ta constituents are 1670°C and 3014°C (3). These high melting temperatures combined with the known reactivity of titanium quickly narrowed the possible melting techniques to those utilizing a water-cooled copper crucible. Other concerns included that the melting point of tantalum (3014°C) was only slightly lower than the boiling point of titanium (3289°C) and that the vapor pressure of Ti is significantly higher than that of Ta. These two concerns eliminated electron beam cold-hearth remelting - although this process is used for the production and refining of both Ti and Ta metal - due to the likelihood of excessive Ti vaporization in the hard vacuum environment. Finally, the large difference in density between titanium and tantalum, 4.5 vs. 16.6 g/cc, and partitioning ratio of 0.8 (for the Ta-Ti system), suggested that micro- or macrosegregation during solidification might be a concern.The melting processes that were selected for evaluation included vacuum arc melting (VAR) and plasma arc melting (PAM). Vacuum arc remelting is used to produce a wide range of materials, including Nb-Ti superconductor alloys (4), Ti alloys, and unalloyed Ta (3-6). Superconductor alloy production of particular interest because the Ti-50 wt% Nb alloy is very similar to the Ti-60 wt% alloy considered here.

Because of the macrosegregation often observedwhen VAR melting Nb-Ti alloys, it was a concern in this study. A comparison of the Ti-Nb and Ti-Ta phase diagrams would suggest equal or greater segregation in the Ti-Ta system. A second consideration is the difficulty in producing and/or attaining complete dissolution of an electrode composed of Ti and Ta metals.

Plasma arc melting (PAM) is frequently used for the consolidation and alloying of Ti and refractory alloys. This process offers the advantages of utilizing a much wider range of feed material, improving dissolution via much higher local superheats, minimizing Ti loss by melting under an inert gas atmosphere, and the possibility of reducing segregation due to the smaller molten pool. The primary concern with plasma melting was obtaining a uniform macrostructure, due to the irregular feed of molten material, smaller molten pool, and relatively high solidification and cooling rates. To address these concerns and investigate the capabilities of alternate melting processes, an initial PAM consolidation step was followed by a matrix of PAM and VAR remelting processes.

EXPERIMENTAL PROCEDURES

A matrix of two-step melting processes were investigated. In all cases, the initial consolidation of Ti sponge and Ta powder was accomplished via plasma melting. The starting material was made up of cold-pressed compacts of the desired composition. In the PAM furnace used in this study, the electrode material is fed horizontally, drip-melted into the crucible. Following initial consolidation, the material was remelted using either the PAM or VAR process. In the case of VAR, the material was double-melted, each melt being a 10cm electrode into a 12cm crucible, a melt rate of approximately 5.4 g/s, and 1.75kA @ (nominal) 22V using drip short control. No magnetic stirring was used. For the PAM remelted ingots, a matrix of four melts were performed.

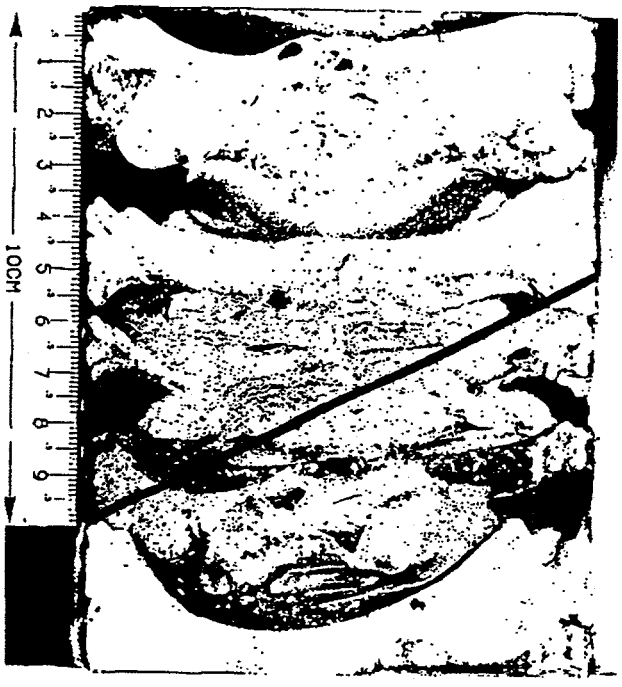

Figure 3. Optical macrograph of initial PAM consolidated ingot.

Two melt rates were used, 4.8 g/s and 9.7 g/s, each with and without magnetic stirring (300A, unidirectional). In all cases, the melts used (nominal) 500A @ 170V and a 10cm crucible. Following melting, all ingots, including the initial PAM consolidated ingot, were sectioned longitudinally, ground, and characterized. Techniques used included optical and electron microscopy, energy-dispersive spectroscopy (EDS), and x-ray fluorescence (XRF) microanalysis. For optical microscopy, the ingots were macroetched using a solution of 30ml HCl, 15ml HNO_3, and 30ml HF.

RESULTS AND DISCUSSION

The initial PAM consolidated ingot is shown in Figure 3, and XRF maps for Ti and Ta are shown in Figure 4. These figures show several things. First, no regions of unmelted Ta were found, indicating that all of the starting powder was melted and some degree of homogenization was achieved. However, as shown in Figure 5, an SEM micrograph, the structure did consist of discrete Ta-rich (85-90% Ta) islands in a matrix having a composition of approximately 45%Ta,

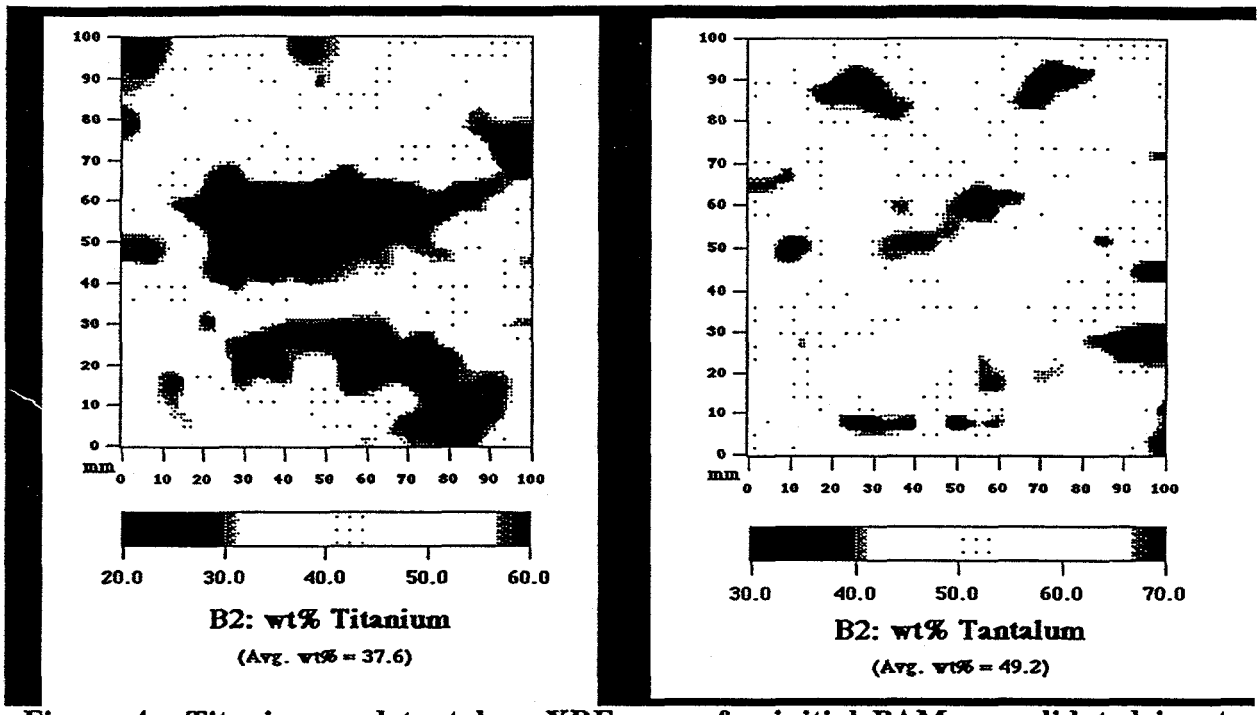

Figure 4. Titanium and tantalum XRF maps for initial PAM consolidated ingot.

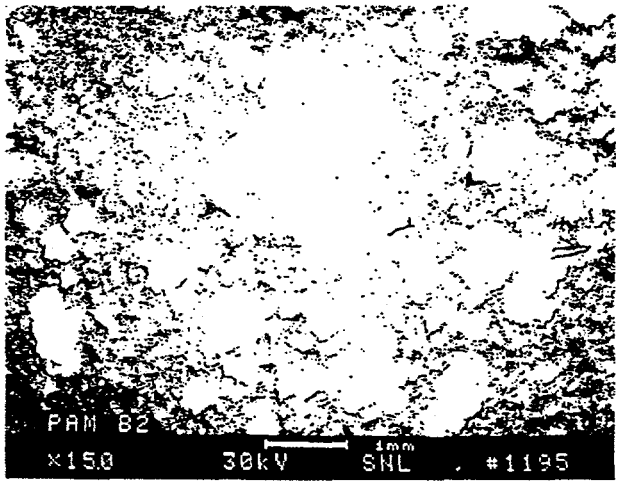

Figure 5. SEM Micrograph of initial PAM consolidated ingot (BSE image).

55% Ti. Figure 3 also shows that the ingot has a layered macrostructure, with numerous voids and cold shuts. This type of ingot macrostructure is not unusual for initial consolidation melts (via plasma or electron beam melting) due to the irregular feed rate and shallow molten pool. The goal of the initial consolidation - to fully melt the starting charge, was achieved.

One method of producing segregation-sensitive Ti or refractory alloys addresses these issues by utilizing a two-step process, consolidation via plasma melting followed by vacuum arc remelting (VAR). Because of the more steady material feed and larger molten pool the VAR remelt step typically maintains a more stable, controlled solidification front. Conversely, the deeper pools can lead to macro- and micro-segregation during solidification, and the minimal superheat in the process limits its ability to dissolve high-melting point inclusions.As a component of this study, a coupled thermal-electrical-fluid numerical simulation (5) of the VAR process was performed to estimate the superheat and molten pool depth. Figure 6 shows the output of this simulation. Figure 6(a) shows a schematic of an ingot with flow streamlines on the left side and temperature contours showing the liquidus, solidus, and a temperature mid-way between the two, on the right. This figure indicates that the molten pool is approximately 0.4 radii, or 2.3 cm (0.9 in) deep, and shows the irregular sidewall often seen in VAR melting of Ti alloys (6). Figure 6(b) shows a plot of temperature along the ingot axis and sidewall. Note that the maximum pool superheat, at the ingot center, is about 32°C, typical of VAR processes (5).

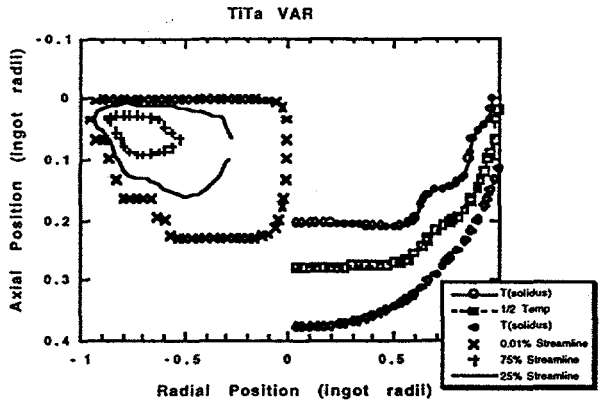

Figure 6(a). VAR model output showing streamlines (left) and liquidus, solidus, and 1/2 way between (right).

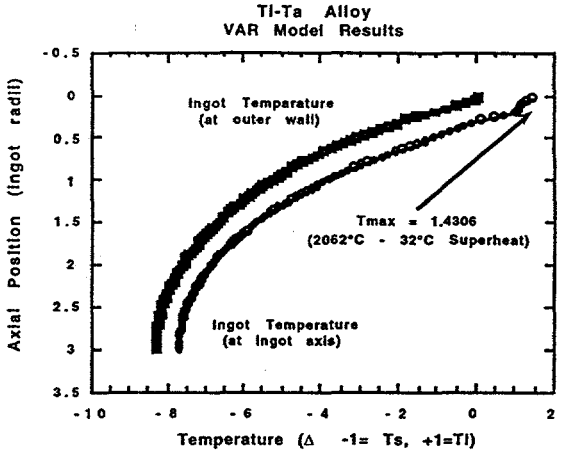

Figure 6(b). VAR model output, ingot axis and wall temperatures. Note that maximum superheat is ~ 32°C.

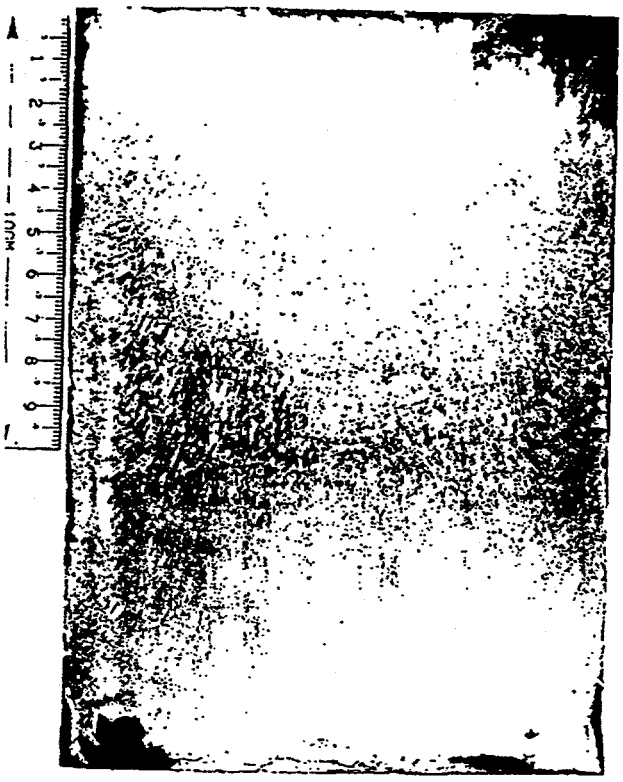

Figure 7. Optical macrograph of PAM consolidated, VAR remelted ingot.

Figure 7 shows the ingot produced by plasma consolidation followed by VAR remelting. In this figure, the pool contours agree with the model prediction of pool depth, and the general macrostructural homogeneity is as expected for this process. Figure 8(a) and 8(b) show a Ta XRF map and line scan for this ingot. These data show that although the VAR remelting greatly improved the macrostructure, it wasn't successful in dissolving the Ta-rich islands in the (plasma consolidated) electrode. Further, the Ta-rich regions are concentrated at the ingot centerline, as would be expected given the deeper melt pool and their greater density than the surrounding material. In the VAR remelted ingot, the matrix composition was higher in Ta than the electrode, 60% Vs 45%, indicating that some of the Ta-rich material went into solution, but the higher Ta regions, those with ≥ 80% Ta, did not. This agrees reasonably well with the model. Figure 2 suggests that a superheat of approximately 50°C is required for significant dissolution of material which is >80% Ta.

A second processing sequence investigated was investigated, involving plasma remelting of the (plasma) consolidated electrode. Four conditions were used, a matrix of 2 melt rates with and without magnetic stirring. The first observation made was that magnetic stirring had little or no effect on either the ingot macrostructure or compositional homogeneity. With respect to melt rate, the results are somewhat mixed. Figure 9(a) and 9(b), XRF maps of the low and high melt rate ingots, respectively, suggest that the higher melt rate ingot may be slightly more homogeneous. Conversely, the ingot macrographs shown in Figure 10 suggest that the low melt rate ingot has a more uniform structure. In both cases, the Ta-rich regions were dissolved to a much greater extent that was the case with VAR remelting -

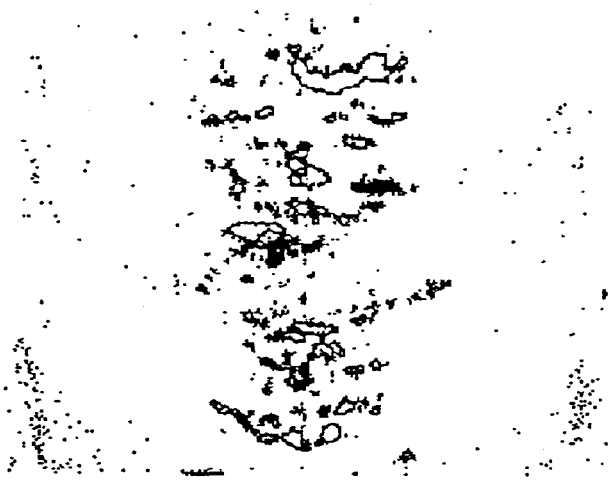

Figure 8(a) Tantalum XRF map for PAM consolidated, VAR remelted ingot.

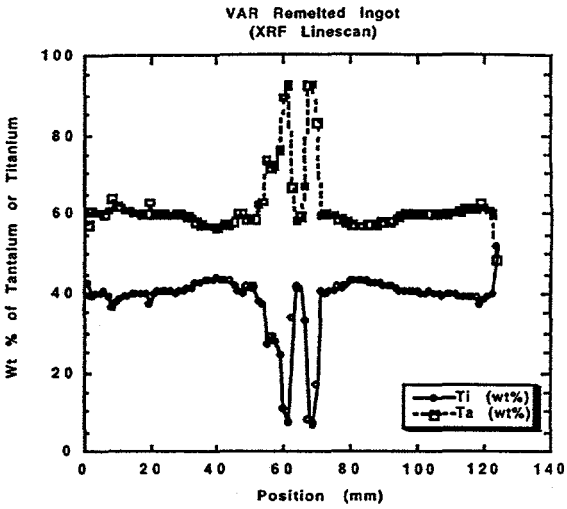

Figure 8(b) XRF Ti and Ta linescans, scanning across ingot shown in 8(a).

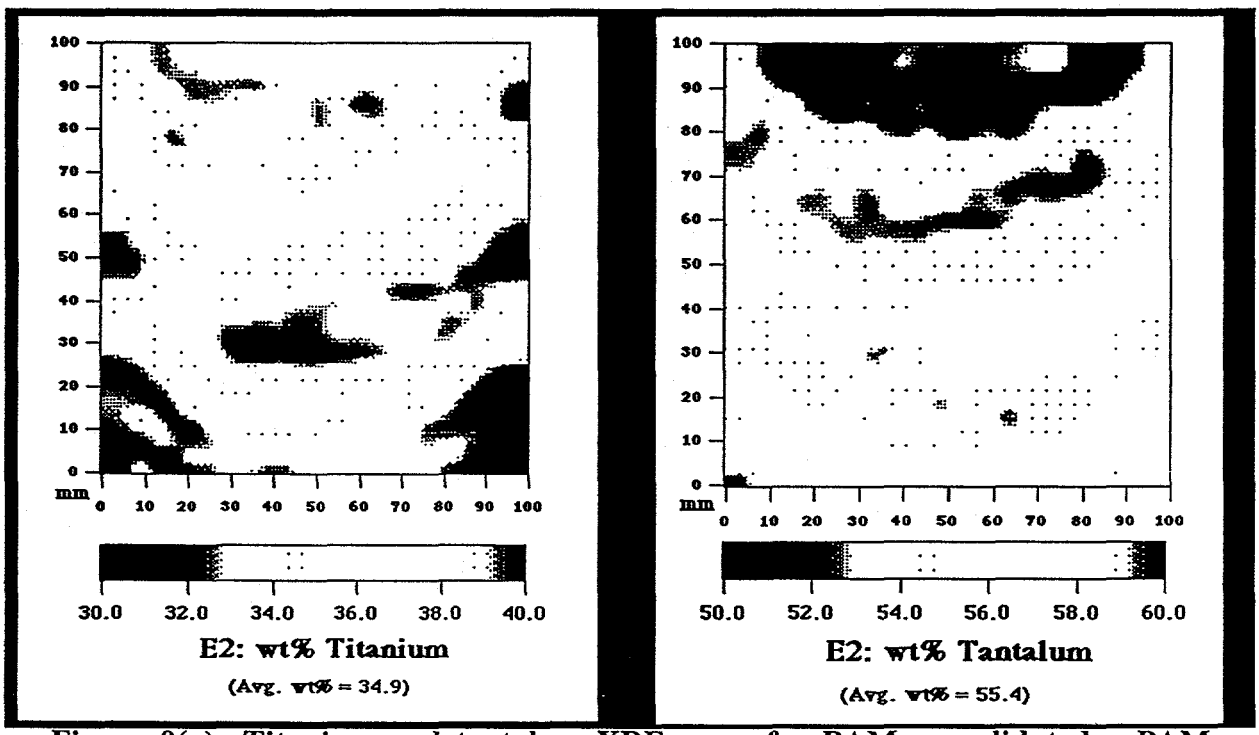

Figure 9(a) Titanium and tantalum XRF maps for PAM consolidated + PAM remelted ingot, made using low melt rate (4.8 g/s) and no magnetic stirring.

consistent with PAM's ability to achieve significantly higher local superheats. Both plasma remelted ingots had a relatively uniform composition of approximately 61% Ta, 39% Ti.

Comparing the microstructures of the ingots produced by the two processes, Figure 11, the grain structure of the plasma ingot is significantly finer that that in the VAR ingot, This is as expected, given the pool is smaller and not directly heated in the plasma process, both contribution to lower local solidification times. Additionally, no microsegregation was detected in the plasma remelted ingot, perhaps due to the finer microstructure. Although the VAR remelted ingot typically showed very little microsegregation, in some regions of the ingot, the dendrite cores were found to be 65-75% Ta and the interdendritic regions, 57% Ta.

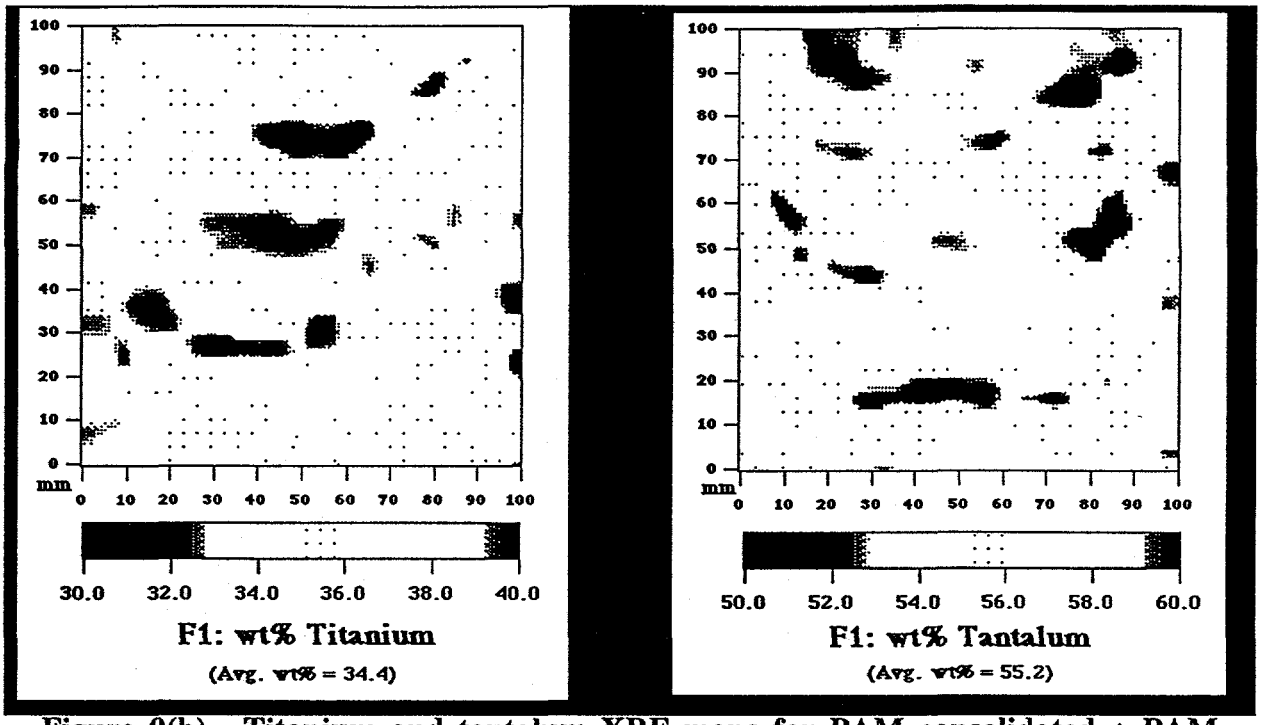

Figure 9(b). Titanium and tantalum XRF maps for PAM consolidated + PAM remelted ingot, made using high melt rate (9.7 g/s) and no magnetic stirring.

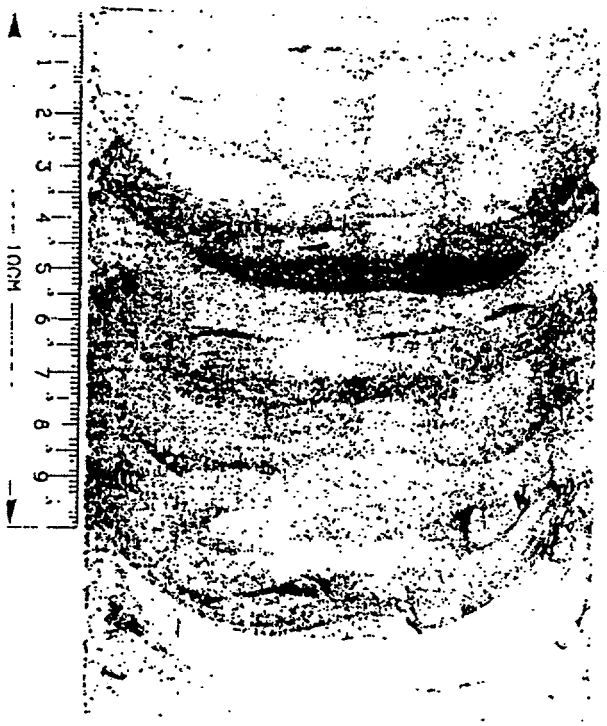

Figure 10. Macrograph of PAM consolidated and remelted ingot (4.8 g/s).

The results of this investigation showed that plasma consolidation, followed by either VAR or plasma remelting, is a viable method for theproduction of this material. To a large degree, the difficulties associated with the differing properties of the starting materials were overcome and a sound, homogeneous ingot of the correct composition could be produced. With respect to the two different processes, the expected limitations and strengths of the selected processes were realized. In the case of VAR remelting, a greater level of structural uniformity was achieved, but the minimal superheat in the process limited its ability to achieve full dissolution of the Ta -rich islands in the electrode. Conversely, the longer solidification times in the VAR process resulted in a slightly coarser microstructure, with a greater degree of microsegregation. Plasma remelting, on the other hand, achieved essentially full dissolution of the electrode material, and a compositionally homogeneous ingot, but resulted in a less uniform ingot macrostructure.These results suggest that that a process utilizing plasma consolidation, a plasma intermediate melt for compositional homogeneity, and a VAR final melt for structure, will produce an optimum ingot. Development and optimization of this process sequence is now the subject of an on-going study.

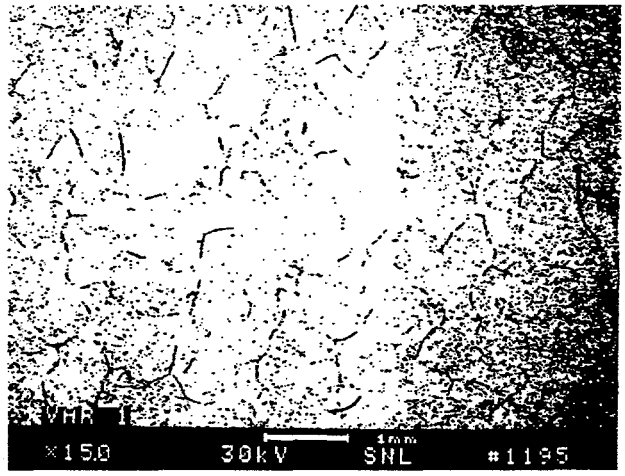

Figure 11(a). SEM micrograph of PAM consolidated + VAR remelted ingot.

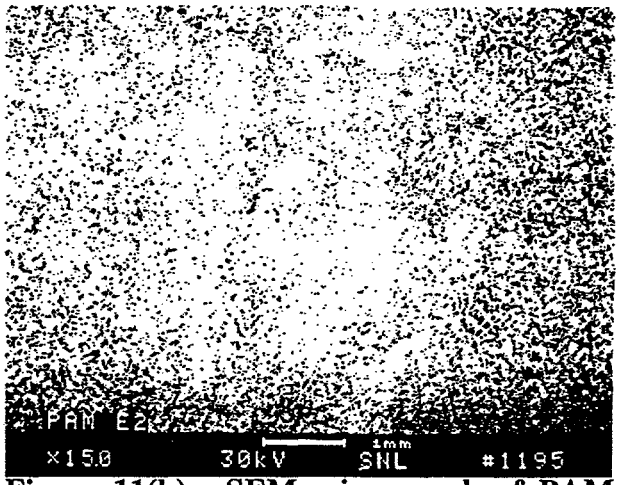

Figure 11(b). SEM micrograph of PAM consolidated + PAM remelted ingot.

CONCLUSIONS

1) Plasma consolidation can achieve complete melting of a Ti-Ta powder starting charge, but not structural or compositional homogeneity.

2) Plasma consolidation, followed by VAR remelting achieves structural homogeneity, but not full dissolution of Ta-rich electrode regions due to the processes limited superheat.

3) Plasma consolidation, followed by plasma remelting, produces a macroscopically homogeneous ingot, but because of the small molten pool and nonuniform feed, one that isn't as structurally uniform as with VAR remelting.

4) Although both processes produced a relatively uniform microstructure, plasma remelting results in a finer ingot grain size.

5) A three-step process, involving plasma consolidation, plasma remelting, and VAR final remelting appears to offer the possibility of producing an optimum ingot.

LIST OF REFERENCES

1) Prokoshkin, D.A., Voronova, T.A., and Gorbova, A.S. "kinetics of Oxidation of Ta-Ti Alloys," Iz. Akad. Nauk. SSSR (Metally), 5, (1984), 178-180.
2) Cotton, J.D., et al. "Nature of Dissolution of Binary Tantalum-Titanium Alloys by Molten Plutonium", in Actinide Processing: Methods and Materials, B. Mishra, ed., (1994), p45. TMS, Warrendale, PA.
3) Murray, J.L. "The Ta-Ti System", Bulletin of Alloy Phase Diagrams, 2(1), (1981). p62.
4) Kreilick, T.S., et al. "Niobium-Titanium Superconductors", Metals Handbook, Volume 2, (1979), p1043. ASM International, Metals Park, OH.
5) Bertram, L.A. and Zanner, F.J. "Interaction between Computational Modeling and Experiments for Vacuum Consumable Arc Remelting", in Modeling of Casting and Welding Processes, H.D. Brody and D. Apelian, eds., (1981), p333. TMS, Warrendale, PA.
6) Hans, S., Jardy, A., and Ablitzer, D. "A Numerical Model for the Prediction of Transient Turbulent Fluid Flow, Heat Transfer and Solidification during Vacuum Arc Remelting" in Proc. of the Vacuum Metallurgy Conference, A. Mitchell and J. Fernihough, eds., (1994), p152. VMD/AVS, New York, NY.